Catalysis Letters Vol. 100, Nos. 1–2, March 2005 (© 2005)
DOI: 10.1007/s10562-004-3078-9

Cerium promoted and silica–alumina supported molybdenum oxide in the zeolite-containing hybrid catalyst for the selective deep catalytic cracking of petroleum naphthas

Nabil Al-Yassir, Raymond Le Van Mao*, and Francine Heng

Industrial Catalysis Research Laboratory and Laboratories for Inorganic Materials, Department of Chemistry and Biochemistry, Concordia University, 7141 Sherbrooke West, SP 275-09, Montreal, Quebec, H4B 1R6 Canada

Received 27 September 2004; accepted 15 November 2004

The high performance of hybrid catalysts in the selective deep catalytic cracking of *n*-hexane and *n*-heptane – used herein as model molecules for petroleum naphthas – is due to the pore continuum effect created by the close connection between the micropores of the acidified silicalite crystallites and the mesopores of the cocatalyst particles, located in fixed positions within a rigid matrix. The resulting enhanced conversion over the "micro–meso" hybrid catalyst is obtained regardless of the surface composition of the mesoporous cocatalyst or the molecular nature of the feed. However, it disappears when the two catalyst components are both mesoporous materials, i.e. in the case of a "meso–meso" hybrid catalyst. The main active component of the mesoporous cocatalyst, molybdenum oxide supported on silica–alumina, shows surface acidity of both nature (Bronsted and Lewis). Cerium oxide incorporated as dopant, has as main catalytic effect to increase the selectivity to light olefins, while the production of aromatics significantly decreases. However, when the ratio of [Ce]/[Mo] molar concentrations is higher than 0.8, the yield of product BTX aromatics rapidly increase at the expenses of that of light olefins. On the other hand, Ce loading onto the microporous silicalite or ZSM5 zeolite results in the same catalytic behavior as with the cerium-doped cocatalyst.

KEY WORDS: hybrid catalysts; selective deep catalytic cracking; silica–alumina; molybdenum; cerium.

1. Introduction

The selective deep catalytic cracking process (SDCC) of petroleum naphthas for the production of light olefins makes use of hybrid catalysts. These materials contain a silica-rich ZSM-5 type zeolite whose submicron-sized particles are intimately mixed with those of a mesoporous cocatalyst, the resulting solid mixture being subsequently extruded with a compressing clay-type binder [1,2]. A recent work (Le Van Mao *et al.*, submitted) has provided clear experimental evidence of the pore continuum effect owing to the close connection of the two differently sized pore openings, which was hypothesized some years ago [3]. The formation of the funnel-shaped pore configuration resulting from this close connection between a microporous pore opening and a mesoporous one under the compressing effect of a clay matrix, results in the suppression of the energy barrier which usually slows down the inward or outward diffusion of reactant or product molecules through the microporous opening of the zeolite particle (Le Van Mao *et al.*, submitted, [3]). In a more specific way, if the particles of the microporous component (pentasil-type H-Silicalite) were solely mechanically mixed with those of the mesoporous component (cocatalyst obtained by supporting molybdenum oxide on silica–alumina (SiAl)), there was almost no change in the conversion of *n*-hexane and in the product selectivities (Le Van Mao *et al.*, submitted). However, if the fine powders of the H-Silicalite and the cocatalyst were at first thoroughly mixed and then embedded (by extrusion and subsequent activation at high temperature) in an extremely rigid solid matrix of bentonite clay, the *n*-hexane conversion over the resulting hybrid catalyst experienced significant increases – up to 55 % – while the sum of the selectivities of the main products of the carbenium-induced cracking (light olefins (+) aromatics) remained unchanged. This effect which was related to the higher rates of diffusion of product (and also reactant) molecules, was supported by the adsorption and desorption data of nitrogen which adsorbed or desorbed in much faster way with the hybrid configuration than with the corresponding mechanical mixture (Le Van Mao *et al.*, submitted). In addition, to express the maximum pore continuum effect, the submicron-sized H-Silicalite particles should be in such a proportion so that they could cover and firmly stick to the external surface of the large cocatalyst particles, thus forming an optimum (hybrid) configuration also called "optimally sparsed structure" by El-Nafaty and Mann [5].

The objectives of this work were as follows:

(a) To confirm the results previously obtained with hybrid catalysts, i.e. improved catalytic performance as a consequence of the formation of a pore continuum in the catalyst rigid matrix, and this in all

---

*To whom correspondence should be addressed.

circumstances provided that the catalysts are prepared from a microporous zeolite and a mesoporous cocatalyst. Different surface composition of the cocatalyst and different feeds (*n*-hexane and *n*-heptane) would be studied;

(b) To investigate the cases of hybrid catalysts whose components were both mesoporous materials; and

(c) To show the important role of the cerium dopant.

2. Experimental

2.1. Preparation of catalysts

2.1.1. Microporous materials

H-Silicalite (HZ): The H-silicalite was prepared by mixing 10.0 g of HISIV 3000 (Molsieve adsorbent) from UOP with 50 mL of NH_4Cl (10% solution). The resulting suspension was stirred for ca.12 h at room temperature and let settled down for 1 h. The mixture was then filtered and the resulting solid was mixed again with NH_4Cl (10% solution) and stirred for ca. 12 h at room temperature. The suspension was again filtered by vacuum (without washing) and the resulting solid was dried overnight at 120 °C and then activated at 500 °C far 3 h. The obtained H-Silicalite had the following physicochemical properties: Si/Al≈217, surface area: 369 m^2/g and microporosity: 136 m^2/g. This material is referred to as HZ.

H-ZSM5 zeolite: The ZSM5 zeolite, herein used as reference, was the Zeocat PZ-2/50H, H-form, powder, purchased from Chemie Uetikon AG (Switzerland). It was activated in air at 500 °C for 3 h. Its main physical properties are: surface area = 454 m^2/g, microporosity = 285 m^2/g and Si/Al = ca.50. This material is referred to as H-ZSM5.

Ce–HZ (y) and Ce/H-ZSM5 (y): The loading of cerium on the zeolites (either H-ZSM5 or H-Silicalite) was conducted by ion-exchange. The exchange by the Ce^{3+} ions was carried out by treating HZ with aqueous solutions of cerium (III) nitrate hexahydrate at different concentrations in CeO_2(y wt%) in the following conditions: 10 g of HZ per 50 cm^3 of solution at moderate stirring for 3 h at 25 °C. It is worth noting that we prefer to express the concentration of the exchange solution or the composition of the final catalysts in CeO_2 because this is the oxidation state of the cerium oxide obtained by calcination at high temperature. After the exchange, the catalyst was filtered (without washing), then dried overnight at 120 °C and calcined in air at 500 °C for 3 h. The preparation of Ce–HZ samples with a solution of concentration in CeO_2 higher than 7.0 wt% was slightly different; HZ or H-ZSM5 was treated twice with the exchanging solution in the same conditions.

2.1.2. Mesoporous materials

Molybdenum and Cerium-based cocatalyst (Cocat): A solution of 8.5 g of ammonium molybdate hexahydrate (Aldrich) dissolved in 50.0 mL distilled water was mixed with a solution of 2.7 g of cerium (III) nitrate dissolved in 40 mL distilled water. The resulting solution was homogenously impregnated onto 50.0 g of SiAl (Aldrich, catalyst support grade 135, SiO_2, 86 wt%; Al_2O_3, 14 wt%; surface area, 443 m^2/g). The solid was dried overnight at 120 °C and then activated at 550 °C for 3 h. The resulting solid had the following physicochemical properties: SiO_2, 63.8 wt%; Al_2O_3, 15.3 wt%; MoO_3, 16.7 wt%; CeO_2, 3.8 wt%; surface area, 354 m^2/g; and microporosity, 0 m^2/g. This material (Ce–Mo/SiAl) is referred to as Cocat.

To investigate the effect of the support and various active and doping components of the cocatalyst, the following materials were also prepared: SiAl, Mo/SiAl, Ce/SiAl.

Ce–Mo/SiAl (x): The preparation of Ce–Mo/SiAl was achieved by impregnation method. The preparation was similar to that of molybdenum and cerium-based cocatalyst, except that, the concentration of Ce^{3+} solution was varied in order to achieve different loadings of cerium. (*x*) was the weight concentration % in CeO_2.

Dealuminated CaA and X zeolites: Mesoporous materials were prepared from Al-rich zeolites (CaA and X) by dealumination with ammonium hexafluorosilicate in aqueous solution [5,6]. In particular, the resulting modified CaA (deal-CaA) and X (deal-X) zeolite materials showed homogeneous pore size distribution at 12 nm and 4 nm, respectively. To acidify the deal-X material, lanthanum ions were incorporated into it by ion-exchange [7], resulting in the La/deal-X sample.

2.1.3. Hybrid catalysts

Micro–Meso hybrid catalysts: A series of hybrid catalysts was prepared by admixing the Cocat or its supported active components (mesoporous materials) with the (microporous) H-Silicalite (HZ) in well-defined proportions: 44 wt% for the microporous component and 56 wt% for the mesoporous component. Bentonite clay was used as ‘‘pressurizing’’ binder to form the final solid matrix of the hybrid catalyst.

Meso–Meso hybrid catalysts: These hybrid catalysts were obtained by admixing the (mesoporous) Cocat with another (mesoporous) acidic material (deal-CaA or La/deal-X) in the same proportion as for the micro–meso hybrid catalysts, i.e. 56 wt% for the Cocat. Bentonite clay was used to form the final matrix of the catalyst.

The extrudates of these hybrid catalysts as well as the monocomponent catalysts were obtained by extrusion with bentonite clay (Spectrum products, 20 wt% of the previous solid mixtures). These catalysts were dried in air overnight at 120 °C and then activated in air at 650 °C for 3 h. They are referred to as HZ//Cocat, HZ//Mo–SiAl, etc.

2.2. Catalyst characterization

1. The HZ (H-silicalite, powder) and the Cocat (Ce/Mo–SiAl, powder) were analyzed by atomic absorption spectroscopy for their chemical composition. The cerium wt% in the Cocat (powder) was determined by gravimetry.

2. BET total and micropore surface areas were determined by nitrogen adsorption/desorption, using a Micromeretics ASAP 2000 apparatus.

3. Ammonia adsorption and temperature-programmed desorption (TPD) technique was used for the study of the total surface acidity. To prevent physisorption phenomena, ammonia was adsorbed at 100 °C. The measurement of acid site density was carried out by heating the ammonia treated catalyst at a constant flow rate of nitrogen (ultra high pure) from 100 °C (temperature of ammonia adsorption) to 580 °C. Using a 0.05 N HCl solution that was then back-titrated with 0.1 N NaOH solution in accordance with the method reported in [5].

4. Fourier transform infrared spectra (using a Nicolet Magna IR Spectrometer 500, resolution 4 cm^{-1}) were recorded in the 400–4000 cm^{-1} region using transmission mode (wafers of sample/KBr mixture = ca. 0.020 g). In particular, the nature of the surface acid sites was investigated by chemical adsorption of pyridine onto clean self-bonded sample wafers after an outgassing under vacuum (10^{-2} mbar) at 220 °C for 4 h. The adsorption of pyridine was done at 160 °C for 3 h. Later, the physisorbed pyridine was removed under vacuum at 80 °C for 1 h. The main peaks of interest for the sorbed pyridine are the ones at 1,455 cm^{-1} and 1,546 cm^{-1} that are usually assigned to the Lewis and Bronsted acid sites, respectively [8].

2.3. Experimental set-up

Experiments were performed using a Lindberg one zone tubular furnace. The reactor vessel consisted of a quartz tube 55 cm in length and 1.5 cm in diameter.

Testing procedures and data reporting: *n*-Hexane and *n*-heptane were used as model molecules for the conversion of petroleum naphthas. Liquids, namely *n*-hexane (or *n*-heptane) and water, were injected into a vaporizer using two infusion pumps. In the vaporizer, nitrogen used as a carrier gas was mixed with *n*-hexane (or *n*-heptane) vapors and steam. The gaseous stream was then sent into the tubular reactor.

The testing conditions were as follows: Weight of catalyst = 2.5 g, weight hourly space velocity (WHSV) = grams of reactant, i.e., *n*-hexane or *n*-heptane injected per hour per gram of catalyst = 1.52 h^{-1}, water/hydrocarbon molar ratio = ca. 0.5 (0.11 g/g), nitrogen flow rate = 3.0 ml/min, duration of the run = 5 h.

Gaseous and liquids were collected separately using a system of condensers. The gas-phase components were analyzed using a Hewlett-Packard 5890 FID gas chromatograph equipped with a 30-m-long GS-alumina micropacked column (J & W Scientific), while the liquid phase analysis was carried out using a Hewlett-Packard 8790 FID gas chromatograph equipped with a 50-m-long PONA capillary column.

The total *n*-paraffin conversion (mol% or wt%) is expressed as follows:

$$C_t(\text{mol or wt\%}) = (\text{moles of converted } n\text{-paraffin}/\text{moles of } n\text{-paraffin fed}) \times 100$$

The selectivity (to product *i*) is expressed as follows:

$$S_i(\text{wt\%}) = (\text{number of C atoms of product } i/\text{number of C atoms of products}) \times 100$$

3. Results and discussion

Table 1 reports some textural and surface acidity properties of the main single component and the "micro–meso" hybrid catalysts used in this work. It is worth noting that commercial Silicalite and ZSM5 zeolite materials are sold in fine powder forms comprising of submicron-sized particles (the smaller the

Table 1

Textural properties and (total) surface acidity of the hybrid catalyst and its single component (all analyzed as extrudates in 20% bentonite, activated at 650 °C)

Catalyst	BET surface area (m^2 /g)	Pore characteristics	Density of acid Sites	
			(mmol/g)	(μ mol/m^2)
HZ (H-Silicalite)	398	Micro	0.313	0.786
H-ZSM-5	454	Micro	1.22	2.68
SiAl	442	Meso	0.698	1.58
Mo/SiAl	349	Meso	1.00	2.87
Ce/SiAl	402	Meso	0.728	1.81
Cocat [Ce–Mo/SiAl (2.2)]	335	Meso	0.944	2.82
Hybrid catalyst (Hyb)	276	Micro–Meso	0.532	1.93

particle size, the larger the external surface area), i.e. also that a significant proportion of the pores of these materials have sizes much larger than 0.55 nm These (small) mesopores presumably correspond to defectuous pores or large pore mouths. On the other hand, it can be seen that, in terms of acid sites density, the Mo/SiAl sample was more acidic than the "active" support SiAl because of the acidity of incorporated MoO_3 [9] which was predominantly of Bronsted nature (table 2 and figure 1). The incorporation of Ce did not seem to affect the total acid sites density (table 1); however, since Ce oxides are known for their slight basic character, it was not surprising that the Bronsted acid sites of the support SiAl were nearly completely neutralized, while the number of Lewis acid sites seemed to increase significantly (table2 and figure 1). However, a detailed study of these sites by using a more selective probe molecule (dimethylpyridine) revealed that Ce species acted rather as adsorption sites capable of binding to the basic probe molecules such as pyridine or dimethylpyridine than "real" Lewis acid sites (Al-Yassir and Le Van Mao, unpublished). Figure 2 shows that most of the Bronsted acid sites of the H-Silicalite were "free" protons (with the same configuration as a supported mineral acid, HCl), which resulted from the decomposition of some ammonium chloride left inside the silicalite after the ion-exchange operation.

The incorporation of Mo onto the SiAl active support significantly increased the total conversion (table 3) owing to the already mentioned increase of the density of acid sites (table 1). However, the product selectivities changed in an important manner (table 3): lower selectivity in light olefins (particularly ethylene and propylene) and higher selectivity in aromatics (particularly in BTX aromatics. i.e. benzene + toluene + xylenes + ethylbenzene).

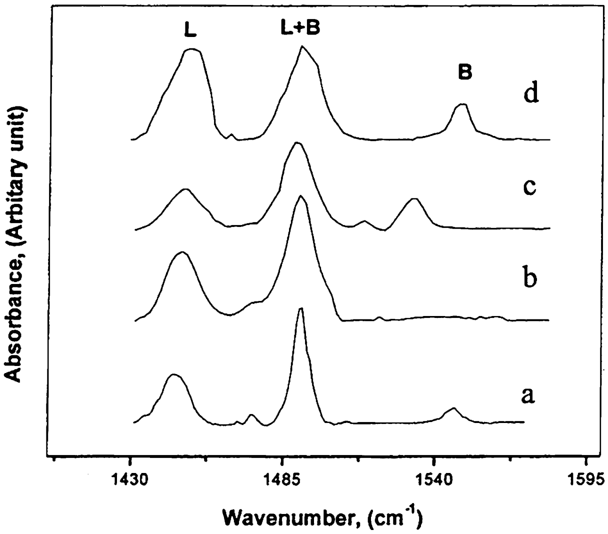

Figure 1. FT-IR spectroscopy of chemisorbed pyridine on (a) SiAl catalyst support; (b) Ce/SiAl; (c) Mo/SiAl; (d) Ce–Mo/SiAl.

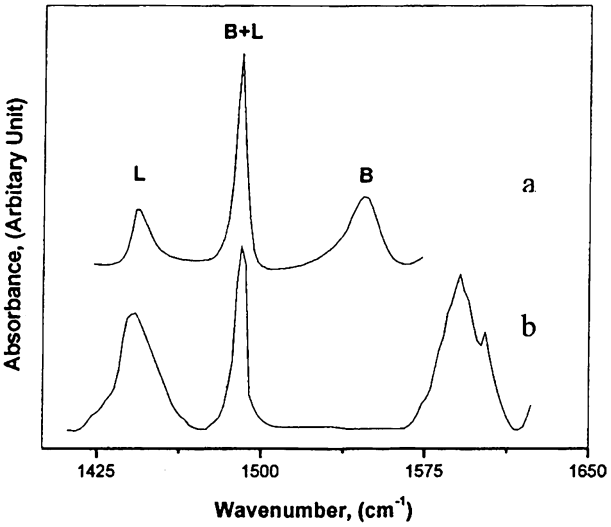

Figure 2. FT-IR spectra of chemisorbed pyridine on (a) H-ZSM-5 & (b) H-Silicalite (HZ).

Loading Ce resulted in exactly the reverse situation (table 3): slightly lower conversion owing to the slightly basic character of CeO_2, higher selectivity to light olefins and significantly lower selectivity to aromatics. Such trends had been already observed by several researchers [10,11]: "...basic sites were newly generated on the catalyst surfaces by the rare earth loading although the acid character of the catalyst was mostly not affected by the modification. The inhibition of olefin adsorption by loaded rare earth metal oxides was assumed to be the major cause of the lower aromatic formation" [12]. Similar effect produced by the newly incorporated "sorption" sites, which were capable of removing the

Table 2

Ratios of FT-IR Bronsted (B) and Lewis (L) peak areas (arbitrary units), obtained by pyridine absorption (for comparison purpose, the extinction coefficients were ignored)

Catalyst	Bronsted Acid sites (B)	Lewis Acid sites (L)	B/L
HZ (H-Silicalite)	6.96	5.16	1.35
H-ZSM-5	6.46	3.24	2.0
SiAl	2.16	9.85	0.22
Mo/SiAl	5.29	10.14	0.52
Ce/SiAl	0.0	6.15	0.0
Cocat [Ce–Mo/SiAl (2.2)]	6.10	23.9	0.26

Table 3
Catalytic properties of the single component catalysts and their corresponding (micro–meso) hybrid catalysts

Catalyst	Feed	Total conversion C_t (wt%)	Product selectivity, S_i (wt%)	
			Ethylene + Propylene	BTX aromatics
HZ (H-Silicalite)	*n*-Hexane	28.9	60.0	0.7
SiAl	*n*-Hexane	27.2	62.9	0.4
Mo/SiAl	*n*-Hexane	35.0	57.0	3.9
HZ//Mo/SiAl	*n*-Hexane	46.8	53.9	4.8
Ce/SiAl	*n*-Hexane	23.4	63.9	0.0
HZ//Ce/SiAl	*n*-Hexane	28.8	57.5	0.6
Ce–Mo/SiAl (Cocat)	*n*-Hexane	30.8	61.1	2.1
HZ//Cocat	*n*-Hexane	55.3	57.8	3.2
HZ	*n*-Heptane	38.0	54.8	0.3
Cocat	*n*-Heptane	39.0	48.6	3.7
HZ//Cocat	*n*-Heptane	54.0	52.2	2.0

Table 4
Catalytic properties of the single component catalysts and their corresponding (meso–meso) hybrid catalysts (feed = *n*-hexane)

Catalyst	Total conversion C_t(wt%)	Product selectivity, S_i (wt%)	
		Ethylene + Propylene	BTX aromatics
Ce–Mo/SiAl (Cocat)	30.8	61.1	2.1
deal-CaA	30.3	62.6	0.6
Cocat//deal-CaA	30.3	62.9	0.9
La-deal-X	30.5	64.1	0.4
Cocat//La-deal-X	27.2	56.7	0.5

Table 5
Catalytic properties of the mesoporous catalysts based on Mo supported on SiAl with various Ce loading (feed = *n*-hexane)

Catalyst	[Ce]/[Mo]	Total conversion C_t (wt%)	Product selectivity, S_i (wt%)	
			Ethylene + Propylene	BTX aromatics
Mo/SiAl	0.00	35.0	57.0	3.9
Ce–Mo/SiAl (0.3)	0.04	34.8	60.6	3.7
Ce–Mo/SiAl (2.2) or Cocat	0.27	30.8	61.1	2.1
Ce–Mo/SiAl (5.0)	0.60	30.8	62.1	1.5
Ce–Mo/SiAl (7.0)	0.85	31.6	61.9	1.3
Ce–Mo/SiAl (10)	1.21	41.5	52.4	5.9
Ce–Mo/SiAl (15)	1.81	38.2	51.9	8.6

carbenium ions, thus shortening their residence time on the acid sites, was also observed with Zn species in the isomerization of *n*-heptane [12].

The dramatic increase in the conversion when the micro–meso hybrid catalysts were used (table 3), could be seen as a new experimental evidence of the effect of the pore continuum as proposed in our previous papers [1–3, Le Van Mao *et al.*, submitted]. This was true for both *n*-hexane and *n*-heptane used herein as model molecules for the selective deep catalytic cracking of naphthas [1,2]. Other convincing results were provided by the meso–meso hybrid catalysts (Table 4): the absence of any significant change in conversion and product selectivities could be interpreted as due to the absence of the need for diffusion enhancement within the totally mesoporous hybrid catalyst matrix.

Thus, Ce species incorporated in limited amounts into the supported molybdenum oxide catalyst favored the production of light olefins, while decreasing the formation of aromatics (table 5). However, an excess of Ce loading resulted in a reverse trend (Tables 5 and 6), suggesting that an important presence of Ce species might lead to the formation of segregated CeO_2 which is known to have strong redox properties [13]. Probably, aromatization occurred over these fine CeO_2 particles still bound to the acidic molybdenum oxide. Such a change in the catalytic behavior happened at a [Ce]/[Mo] molar ratio of 0.7–0.8 (table 5). It is worth mentioning that a [Ce]/[Mo] molar ratio of ca 0.7 corresponds to the stable compound $Ce_2(MoO_4)_3$ which can promote the selective oxidation of toluene to benzaldehyde [14].

Table 6
Catalytic properties of the catalysts based on the microporous H-Silicalite and H-ZSM-5, with various Ce loading (feed = *n*-hexane), ^{a}CeO$_2$ concentration of the exchanging solution

Catalyst	Ce concentration[a]	Total conversion C_t (wt%)	Product selectivity, S_i (wt%)	
			Ethylene + Propylene	BTX aromatics
HZ	0.00	28.9	60.0	0.7
Ce–HZ (0.3)	0.3	25.9	60.9	0.3
Ce–HZ (2.2)	2.2	25.4	61.3	0.2
Ce–HZ (5)	5.0	25.0	61.9	0.1
Ce–HZ (7)	7.0	27.8	61.5	0.7
Ce–HZ (10)	10.0	28.0	60.9	0.9
Ce–HZSM-5	0.00	94.7	50.4	5.8
Ce–HZSM-5 (0.32)	0.3	92.9	51.5	5.4
Ce–HZSM-5 (2.2)	2.2	89.6	53.5	4.3
Ce–HZSM-5 (5)	5.0	86.2	54.5	3.2
Ce–HZSM-5 (7)	7.0	89.4	53.2	4.9
Ce–HZSM-5 (10)	10.0	90.8	50.5	6.3

4. Conclusion

The high performance of hybrid catalysts used in the selective deep catalytic cracking of *n*-hexane and *n*-heptane was due to the pore continuum effect created by the close connection between the micropores of the acidified silicalite crystallites and the mesopores of the cocatalyst particles, located in fixed positions within a rigid matrix. The resulting enhanced conversion over the "micro–meso" hybrid catalyst was obtained regardless of the surface composition of the mesoporous cocatalyst or the molecular nature of the feed. However, it disappeared when the two catalyst components were both mesoporous materials, i.e. in the case of a "meso–meso" hybrid catalyst.

The main active component of the mesoporous cocatalyst, molybdenum oxide supported on SiAl, showed surface acidity of both nature (Bronsted and Lewis). Cerium oxide incorporated as dopant, had as main catalytic effect to increase the selectivity to light olefins, while the production of aromatics significantly decreases. However, when the ratio of [Ce]/[Mo] molar concentrations was higher than 0.8, the yield of product BTX aromatics rapidly increased at the expenses of that of light olefins.

Acknowledgments

Financial support from NSERC (Natural Science and Engineering Research Council of Canada) and Valeo Management-Quebec is acknowledged. We also thank Mrs. Lu Lan for her technical assistance.

References

[1] R. Le Van Mao R, S. Melancon, C. Gauthier-Campbell and P. Kletnieks, Catal. Lett. 73(2/4) (2001) 181.

[2] S. Melancon, R. LeVan Mao, P. Kletnieks, D. Ohayon, S. Intem, M.A. Saberi and D. McCann, Catal. Lett. 80(3,4) (2002) 103.

[3] R. LeVan Mao, Micropor. Mesopor. Mater. 28 (1999) 9.

[4] U.A. El-Nafaty and R. Mann, Chem. Eng. Sci. 54 (1999) 3475.

[5] R. LeVan Mao, N.T.C. Vo, G. Denes and T.S. Le, J. Porous Mater. 1 (1995) 175.

[6] R. LeVan Mao, G. Denes, N.T.C. Vo, J.A. Lavigne S.T. Le, Mat. Res. Soc. Symp. Proc. 371 (1995) 123.

[7] S. Xiao, R. LeVan Mao and G. Denes, J. Mater. Chem. 5(80) (1995) 125.

[8] J. Lynch, in: *Analyse physico-chimique des catalyseurs industriels*, Edition Technip (Paris, 2001), p. 273.

[9] H.H. Kung, in: *Transition Metal Oxides: Surface Chemistry and Catalysis.*, B. Delmon and J.T. Yates (eds.), (Elsevier Science, Amsterdam, 1989) 83.

[10] F. Lemos, F.R. Ribeiro, M. Kern, G. Giannetto and M. Guisnet, Appl. Catal. 29 (1987) 43.

[11] K. Wakui, K.I. Satoh, G. Sawada, K. Shiozawa, K.I. Matano, K. Suzuki, T. Hayakawa, K. Murata, Y. Yoshimura and F. Mizukami, in: *Studies in Surface Science and Catalysis*, I. Kiricsi, G. Pal-Borbely, J.B. Nagy and H.G. Karge (eds), Vol. 125 (Elsevier Sc. Amsterdam, 1999), p. 449.

[12] M.A. Saberi, R. LeVan Mao, M. Martin and A.W.H. Mak, Appl. Catal. A: General 214 (2001) 229.

[13] J.C. Conesa, M. Fernandez-Garcia and A. Martinez-Arias, in: *Catalysis by Ceria and Related Materials*, A. Trovarelli (eds.), (Imperial College Press, London, 2002) 190–193.

[14] W. Kuang, Y. Fan and Y. Chen, Catal. Lett. 50 (1998) 31.